***Cell*, Volume 135**

Supplemental Data

Real-Time Redox Measurements during Endoplasmic Reticulum Stress Reveal Interlinked Protein Folding Functions

Philip I. Merksamer, Ala Trusina, and Feroz R. Papa

SUPPLEMENTARY EXPERIMENTAL PROCEDURES

Plasmid Construction

The eroGFP gene was generated by ligating the first 135 nucleotides of the *KAR2* ORF to the N-terminus of the ro2GFP ORF (Dooley et al., 2004; Hanson et al., 2004) using Nhe1 and BamH1 restriction sites, and by fusing an HDEL retention sequence to its C-terminus using overlap extension PCR. This gene was then positioned under control of the constitutive TDH3 promoter and the CYC1 terminator. This construct is on pPM28 [*CEN URA3 eroGFP*] used for light microscopy and pPM44 [*integrating NAT eroGFP*] used for flow cytometry in Figure 1. Recombinant eroGFP was made by ligating ro2GFP-HDEL into the pRSETb bacterial expression vector (Invitrogen) (pPM35) using BamH1 and HindIII sites. pPM57 containing eroGFP(C147S) was made by QuickChange site-directed mutagenesis (Stratagene) of pPM44. GAL-eroGFP (pPM60) was made by replacing the TDH3 promoter in pPM44 with the GAL1 promoter using *in vivo* DNA gap repair (Papa et al., 1999). UPR-RFP (pPM47) was made by fusing a tandem 4xUPRE containing *CYC1* promoter upstream of the coding sequence for mCherry by overlap extension PCR. 4xUPRE-Cyc1pr and mCherry containing plasmids were gifts from JS Weissman. pPM48 [*integrating NAT eroGFP-UPR-RFP*] and pPM56 [*integrating KAN eroGFP-UPR-RFP*] were made by overlap

extension PCR. The Ero1-3HA construct was a gift from J.S. Weissman (Pollard et al., 1998). CPY-3HA and CPY*-3HA constructs were derived from plasmids from J.S. Weissman (Bhamidipati et al., 2005) and made by fusing the CUP1 promoter to the coding sequences of pcr1 and pcr1-1 (encoding the CPY or CPY* proteins respectively) on *2μ* shuttle *LEU2* vectors using *in vivo* DNA gap repair—pPM17 [*2μ LEU2 CPY-HA*] and pPM18 [*2μ LEU2 CPY*-HA*]. The non-glycosylated CPY* construct—CPY*0000—(pPM65) was derived from a CPY*0000 containing plasmid from D.T. Ng (Spear and Ng, 2005) and placed under the CUP1 promoter as described above. The single cysteine (pPM66) and cysteine-less CPY* (pPM67) constructs were derived from a CUP1-CPY* construct containing three cysteines from A.A. Cooper (Haynes et al., 2004) and modified by QuickChange site-directed mutagenesis (Stratagene) and cloned into *2μ* shuttle *LEU2* vectors using SacI and XhoI restriction sites. The single cysteine in pPM66 is located at position 167. The constitutive-ON, kinase-dead, 1NM-PP1-sensitized Ire1 plasmid was previously described (Papa et al., 2003). All plasmids were sequenced on both DNA strands.

Pulse Chase of eroGFP

Wild-type cells expressing GAL-eroGFP were grown to mid-log phase in SGal media at which point 2% glucose was added. An equal volume of galactose was added to the control group. After 2.5 hrs cells were washed two times in 1 ml of either SD or SGal without amino acids and resuspended in 150 μl of SD or SGal without amino acids. Cells were pulsed with 20μCi of Tran^{35}S-label (MP Biomedicals) for 15 minutes and chased with SD or SGal supplemented with 10mM methionine for 5 min. Cells were lysed in Triton lysis buffer (150 mM NaCl, 50 mM HEPES pH 7.5, 5mM EDTA, and 1% Triton-X100) with glass bead vortexing. eroGFP was immunoprecipitated with 8 μg/ml of anti-GFP (Invitrogen/Molecular Probes) and anti-rabbit

magnetic beads (Invitrogen) following the manufacture's protocol, with the exception that we only used one instead of the three recommended washes in 5% Normal Goat Serum (NGS) 1%Triton, 3% BSA wash buffer. Equal amounts of supernatant recovered from magnetic beads were loaded in two SDS-PAGE protein gels: one was analyzed by immunoblotting and the other was exposed to Kodak autoradiography film for 5 days after being fixed in 65% Isopropanol, 10% Acetic acid, 25 % water, incubated in Enhance solution (Amersham) for 30 min, and dried at 55^{o}C for 2 hours.

Determination of the Oxidation State of eroGFP and Ero1p

Oxidation state determination was performed as previously described (Frand and Kaiser, 1999). In brief, mid-log phase growing yeast cultures were harvested by centrifugation and resuspended in 15% TCA to precipitate proteins and prevent disulfide exchange. Vortexing with glass beads was used to disrupt the cell wall and membranes. Protein pellets were washed with acetone and were solubilized in 50µl of non-reducing sample buffer containing 80mM Tris-HCl (pH 6.8), 2% SDS, 1mM PMSF, and bromophenol blue. This buffer contained 25mM 4-acetamido-4′-maleimidylstilbene-2,2′-disulfonic acid (AMS, Molecular Probes) when indicated. For analysis of Ero1p-3HA this buffer also contained 6M urea. Samples were incubated on ice for 15 minutes, at 37^{o}C for 10 minutes (for Ero1p only), and boiled for 5 minutes. To deglycosylate Ero1p-3HA, samples were diluted 4-fold into 50 mM sodium citrate (pH 5.5) containing 5 mU of Endoglycosidase H (Roche Diagnostics) and incubated at 37°C for 2.5 hr. Samples were resolved by non-reducing SDS-PAGE and immunoblotted with anti-GFP (1:1000, Invitrogen/Molecular Probes) or anti-HA (1:2000, Rockland) when indicated.

Immunoblots

Yeast protein extracts and immunoblots were performed as previously described (Leber et al., 2004). The following primary antibodies were used: anti-Pdi1p (1:2000, a gift from JS Weissman), anti-Pgk1p (1:5000, Invitrogen/Molecular Probes), anti-HA (1:2000, Rockland), and anti-CPY (1:5000, Abcam).

SUPPLEMENTARY REFERENCES

Bhamidipati, A., Denic, V., Quan, E.M., and Weissman, J.S. (2005). Exploration of the topological requirements of ERAD identifies Yos9p as a lectin sensor of misfolded glycoproteins in the ER lumen. Mol Cell *19*, 741-751.

Dooley, C.T., Dore, T.M., Hanson, G.T., Jackson, W.C., Remington, S.J., and Tsien, R.Y. (2004). Imaging dynamic redox changes in mammalian cells with green fluorescent protein indicators. J Biol Chem *279*, 22284-22293.

Frand, A.R., and Kaiser, C.A. (1999). Ero1p oxidizes protein disulfide isomerase in a pathway for disulfide bond formation in the endoplasmic reticulum. Mol Cell *4*, 469-477.

Hanson, G.T., Aggeler, R., Oglesbee, D., Cannon, M., Capaldi, R.A., Tsien, R.Y., and Remington, S.J. (2004). Investigating mitochondrial redox potential with redox-sensitive green fluorescent protein indicators. J Biol Chem *279*, 13044-13053.

Haynes, C.M., Titus, E.A., and Cooper, A.A. (2004). Degradation of misfolded proteins prevents ER-derived oxidative stress and cell death. Mol Cell *15*, 767-776.

Leber, J.H., Bernales, S., and Walter, P. (2004). IRE1-independent gain control of the unfolded protein response. PLoS Biol *2*, E235.

Papa, F.R., Amerik, A.Y., and Hochstrasser, M. (1999). Interaction of the Doa4 deubiquitinating enzyme with the yeast 26S proteasome. Mol Biol Cell *10*, 741-756.

Papa, F.R., Zhang, C., Shokat, K., and Walter, P. (2003). Bypassing a kinase activity with an ATP-competitive drug. Science *302*, 1533-1537.

Pollard, M.G., Travers, K.J., and Weissman, J.S. (1998). Ero1p: a novel and ubiquitous protein with an essential role in oxidative protein folding in the endoplasmic reticulum. Mol Cell *1*, 171-182.

Spear, E.D., and Ng, D.T. (2005). Single, context-specific glycans can target misfolded glycoproteins for ER-associated degradation. J Cell Biol *169*, 73-82.

Supplementary Figure S1

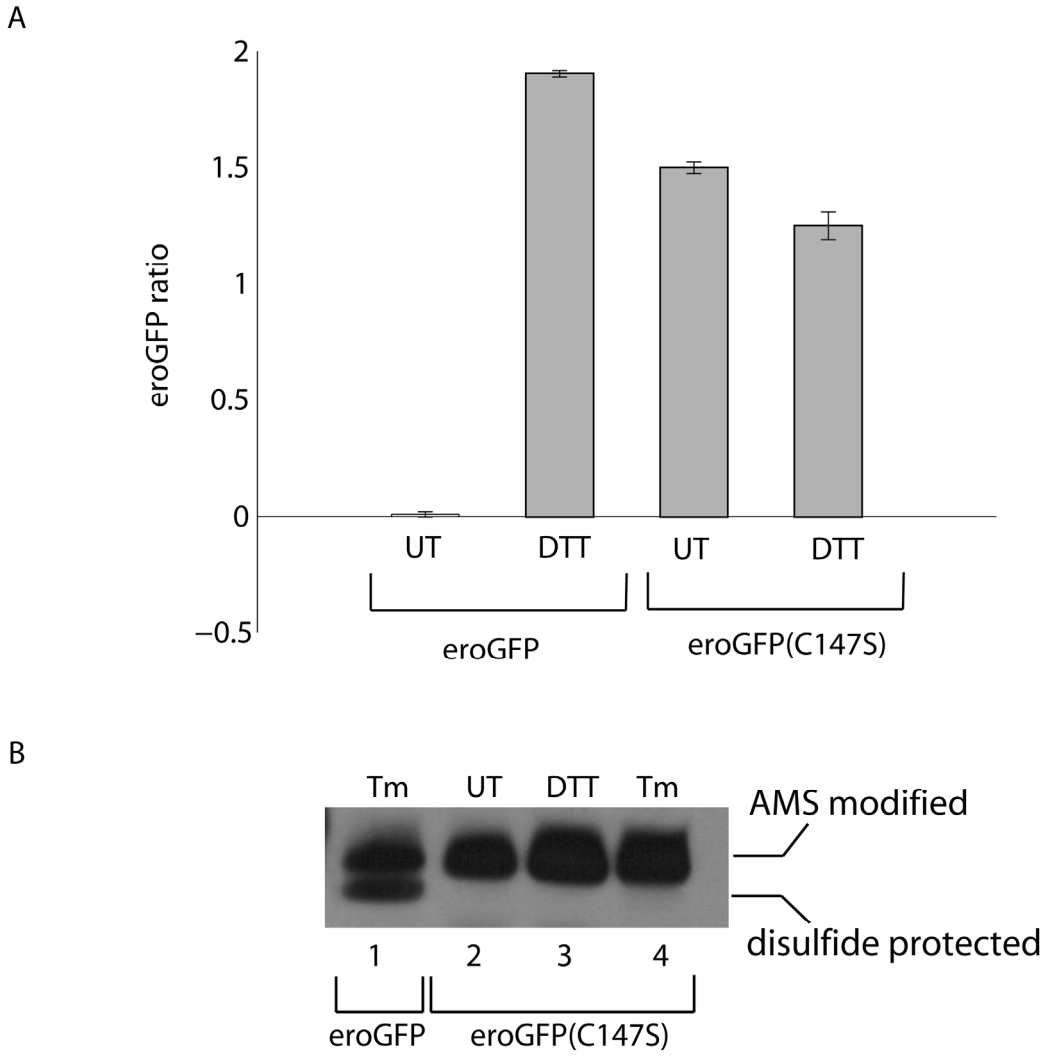

Figure S1. Oxidation changes in eroGFP require a disulfide pair

(A) Wild-type cells expressing eroGFP or eroGFP(C147S) were treated with 4mM DTT for 10 minutes and fluorescence measured by flow cytometery as described in Figure 1. UT indicates untreated. The eroGFP ratio was normalized to the untreated case for wild-type eroGFP. Data represent means +/- SD of three independent experiments. (B) Protein extracts from cells expressing eroGFP treated with 2μg/ml Tm for 3 hours (lane 1) and from cells expressing eroGFP(C147S) untreated (lane 2), treated with 10mM DTT for 10 minutes (lane 3), or treated

with 2μg/ml Tm for 3 hours (lane 4). Extracts were treated with AMS, resolved on non-reducing SDS-PAGE, and immunoblotted against GFP.

Supplementary Figure S2

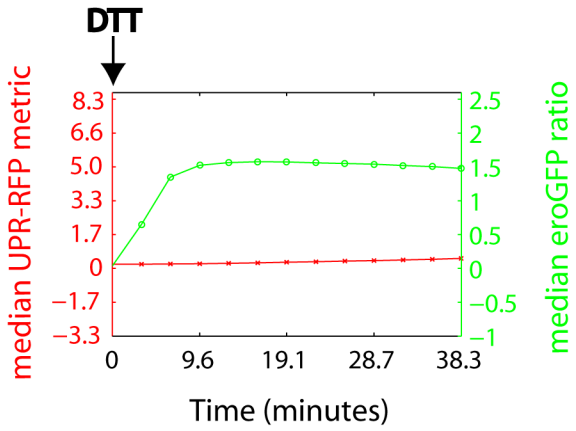

Figure S2. Finer resolution time course of ER redox status and UPR activity for early time points during inhibition of protein oxidation

Time-course of wild-type cells expressing the composite reporter treated with 2mM DTT at time, t=0. Automated sampling was performed every ~3 min for ~40 min. The median eroGFP ratio is represented by green circles and the median UPR-RFP metric is represented by red x-marks.

Supplementary Figure S3

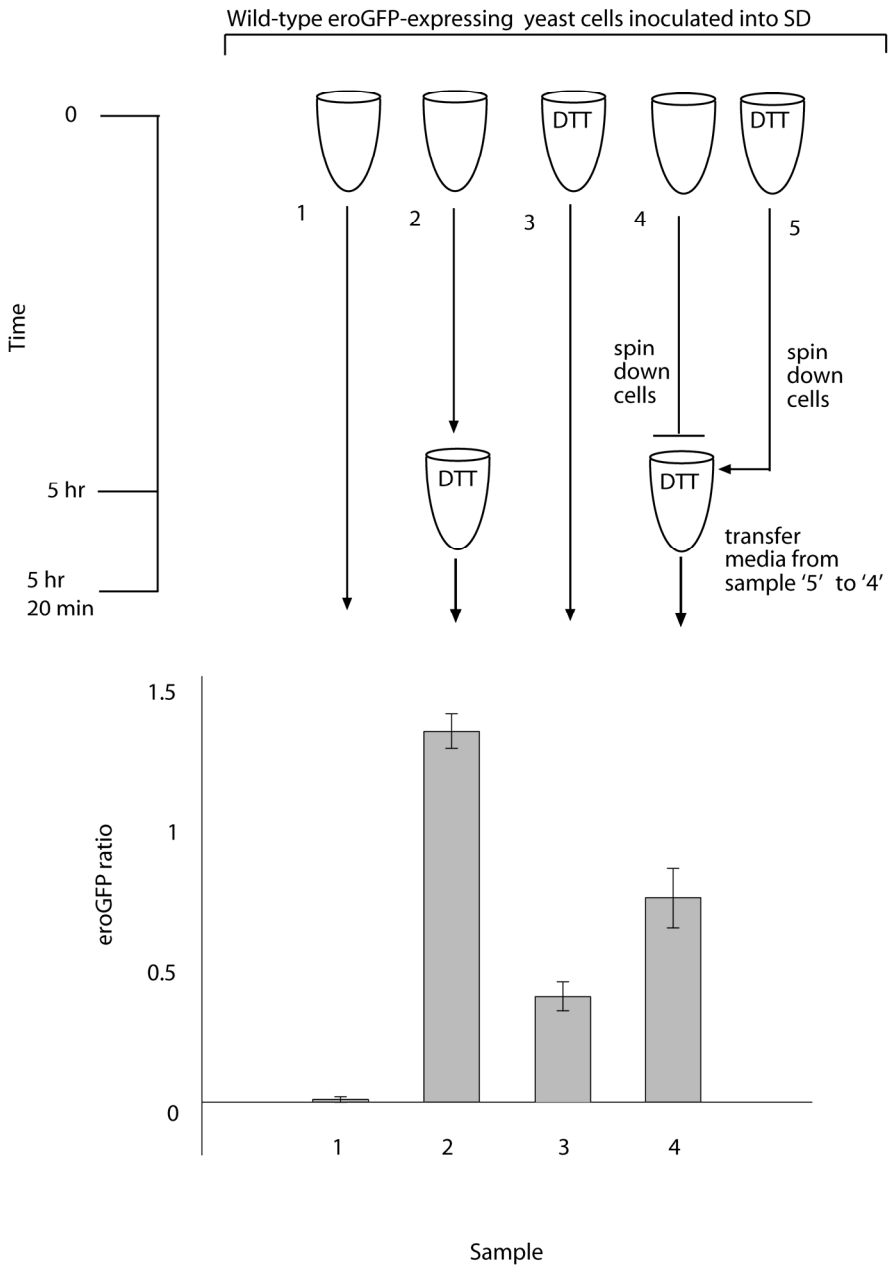

Figure S3. Adaptation to prolonged exposure to DTT

Upper panel: Schematic of experimental design. Wild-type cells expressing eroGFP were inoculated into SD media. At time t=0, samples 3 and 5 were treated with 2mM DTT. At t=5 hrs, sample 2 was treated with 2mM DTT. At t=5 hrs, samples 4 and 5 were centrifuged, media was discarded from sample 4, and cells were resuspended in the media from sample 5. At t=5 hrs 20min, the eroGFP ratio was measured. Lower panel: Bar graph of eroGFP ratio for samples 1-4. The eroGFP ratio was normalized to sample 1. Data represent means +/- SD of two independent experiments.

Supplementary Figure S4

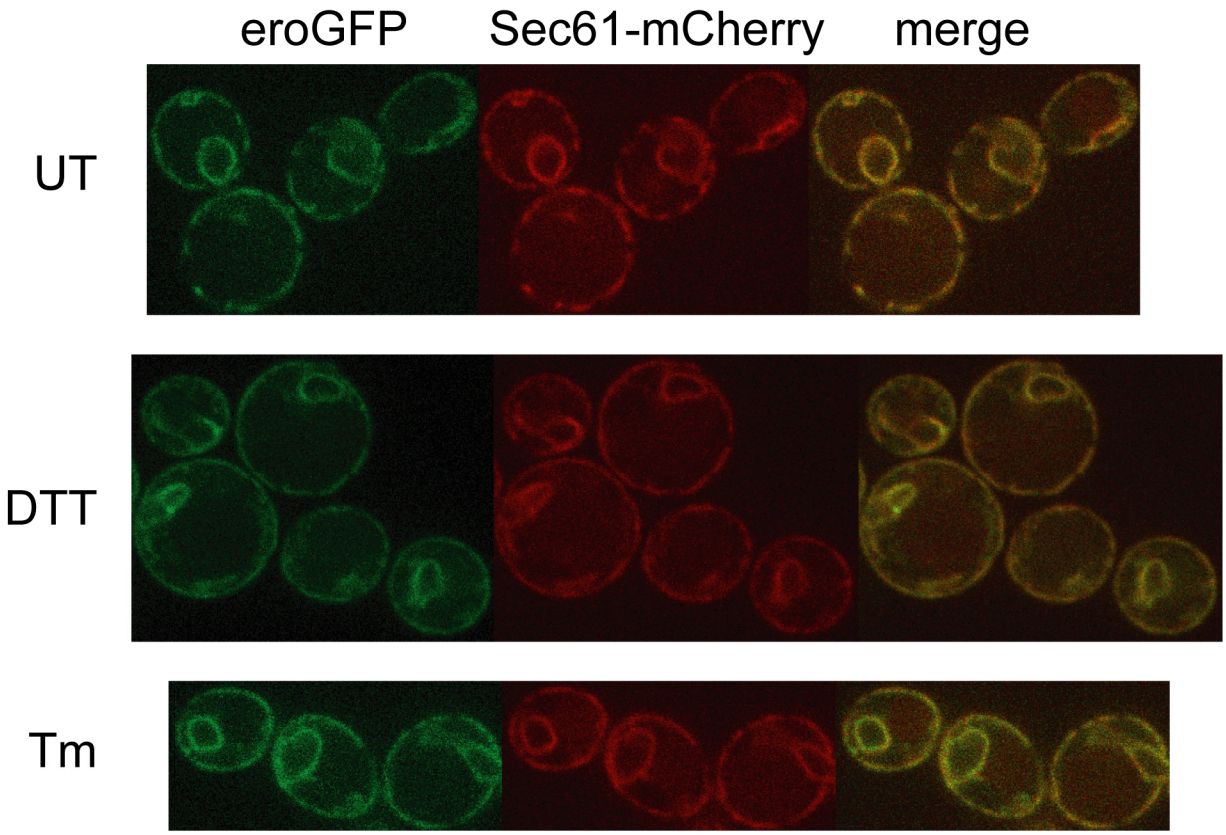

Figure S4. Localization of eroGFP during ER stress

Representative images of cells expressing eroGFP and Sec61-mCherry taken by spinning disk confocal microscopy. UT: untreated. DTT: 2mM DTT for 1 hour. Tm: 1µg/ml Tm for 2 hours.

Supplementary Figure S5

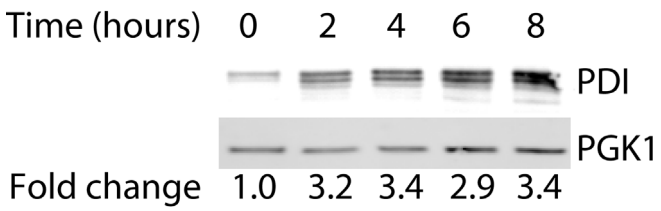

Figure S5. Induction of the ER chaperone and oxidoreductase, PDI, after ER stress

Wild-type cells expressing the composite reporter were treated with 2mM DTT for eight hours. Samples were taken every two hours for SDS-PAGE and immunoblotted against PDI and PGK1, a loading control.

Supplementary Figure S6

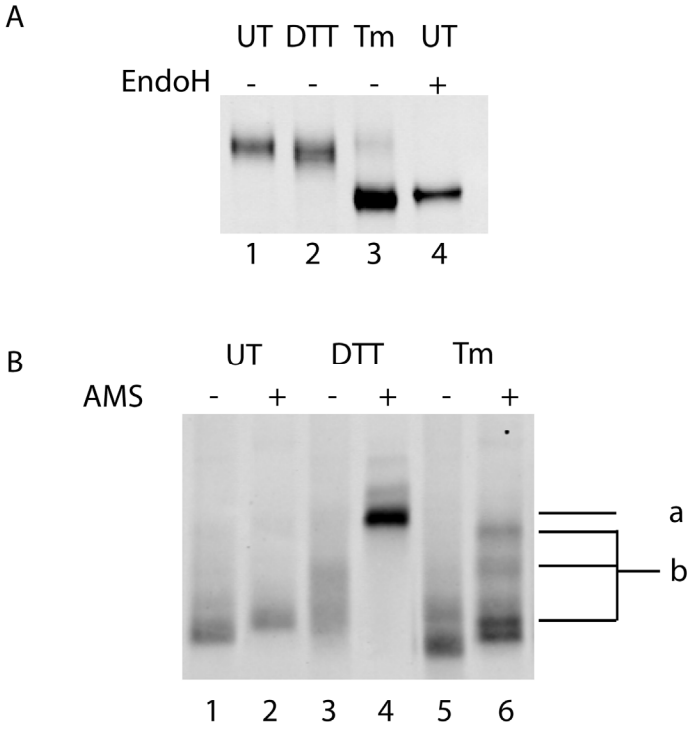

Figure S6. Changes in oxidation state of Ero1p during ER stress

(A) Protein extracts from wild-type cells expressing the composite reporter and Ero1p-3HA were treated with 10mM DTT for 30 min (lane 2), treated with 2μg/ml Tm for 3 hours (lane 3), or untreated (lanes 1 and 4). Extracts in lane 4 were deglycosylated with EndoH. Extracts were resolved on reducing SDS-page and immunoblotted against HA. Note that deglycosylation from Tm treatment produced the same faster migrating species from *in vitro* EndoH treatment of the untreated sample indicating its complete under-glycosylation *in vivo* (lanes 3 and 4). (B) Protein extracts from cells described above were treated with AMS as indicated, followed by treatment with EndoH to deduce mobility shifts due to AMS modification of available sulfhydryls in the different treatments. Samples were then resolved on non-reducing SDS-PAGE, and

immunoblotted against HA. Note the appearance of the AMS modified band due to DTT treatment in lane 4 (marked a), and the three AMS modified bands due to Tm treatment in lane 6 (marked b).

Supplementary Figure S7

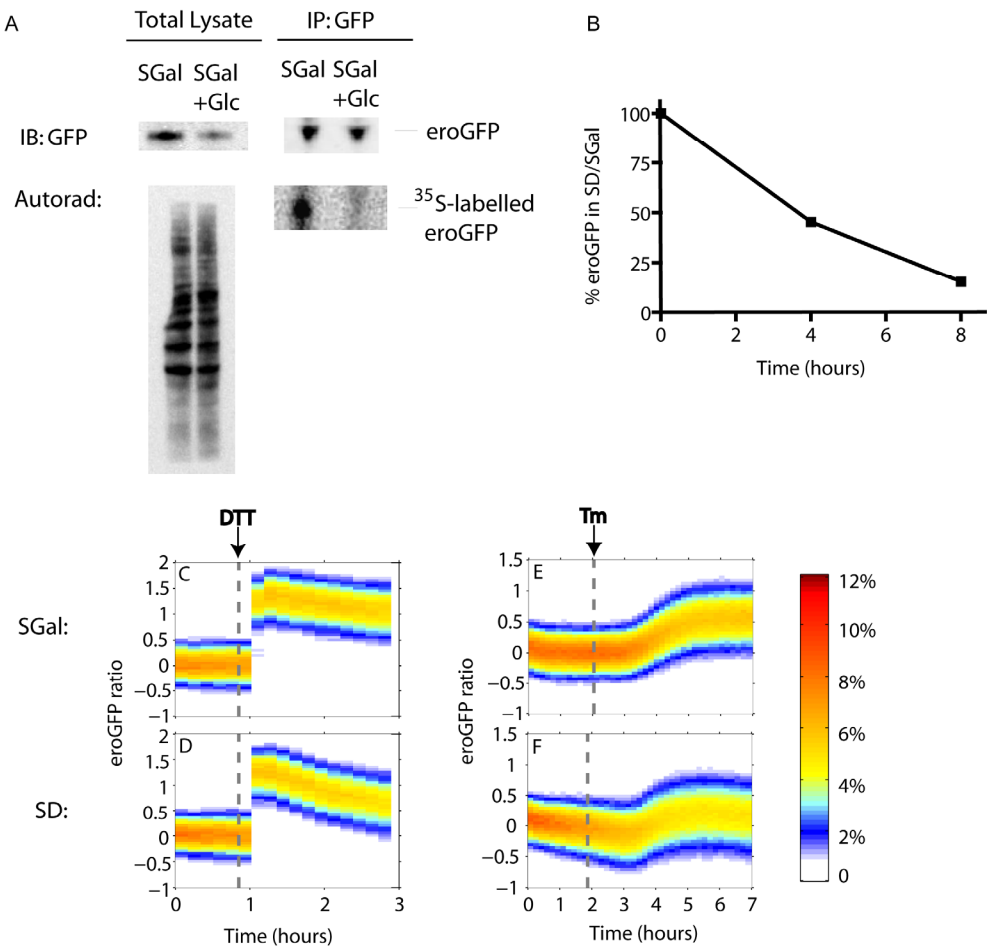

Figure S7. Dynamic monitoring of pre-existing eroGFP redox status during ER stress

(A) Pulse-chase of wild-type cells expressing GAL-eroGFP. See supplementary experimental procedures for details. (B) Quantification of eroGFP protein levels normalized to PGK1 for wild-type cells expressing GAL-eroGFP in SD vs. SGal media. (C-F) Time courses of the eroGFP ratio histograms in wild-type cells expressing GAL-eroGFP during treatment with DTT (2mM) or Tm (1µg/ml). The eroGFP ratio is normalized to unstressed cells. Color represents percentage of cells at a given metric value and time point. Dashed gray line signifies time of stressor addition. Thirty minutes prior to sampling cells growing exponentially in SGal media were diluted 1/30 into SGal media (C) and (E) or SD media (D) and (F). We noted a slightly faster

decay after DTT treatment in (D) vs. (C), possibly due to the lack of newly-synthesized eroGFP requiring oxidation in (D).

Supplementary Figure S8

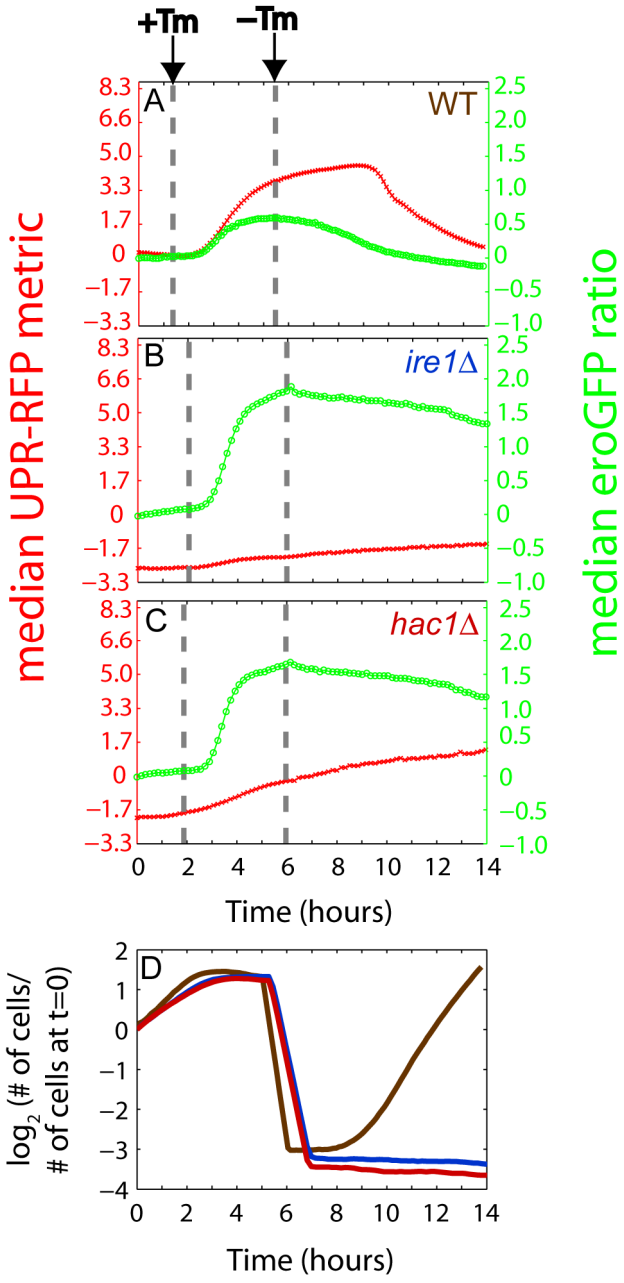

Figure S8. Dynamic monitoring of ER redox status and UPR activity during recovery from glycosylation inhibition

Median values for the eroGFP ratio and the UPR-RFP metric in wild-type (A), *ire1*Δ (B), and *hac1*Δ (C) cells expressing the composite reporter during treatment with Tm (1µg/ml) and during

recovery. The eroGFP ratio is represented by green circles the UPR-RFP metric is represented by red x-marks. The first dashed gray line denotes time of Tm addition and the second dashed gray line denotes time of dilution (1:25) into fresh media. The upward drift of UPR-RFP in the UPR mutants may be due to RFP accumulation in the growth-arrested cells. (D) Growth curves for WT (brown), *ire1*Δ (blue), and *hac1*Δ (red) cells are plotted as the $\log_2$ number of cells normalized to the number of cells at time, t=0. Note that only wild-type cells resume growth upon Tm removal.

Supplementary Figure S9

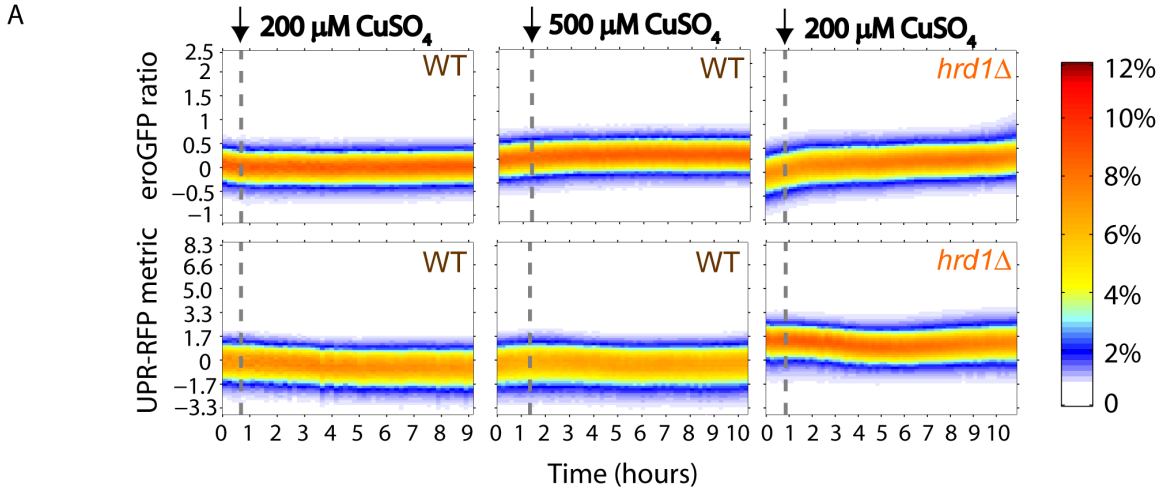

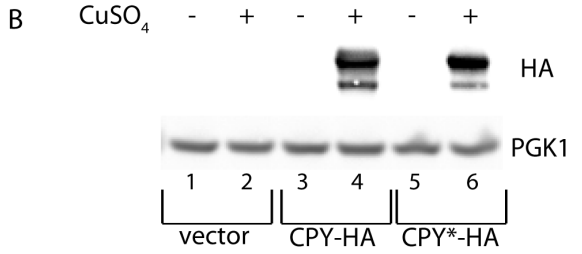

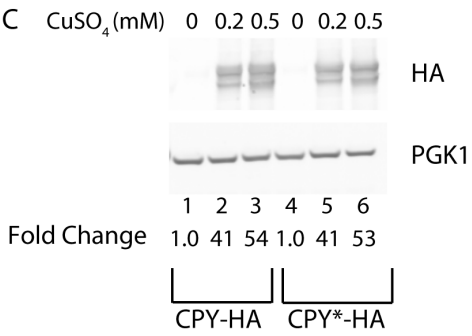

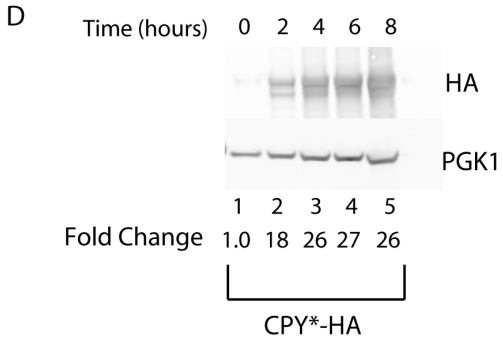

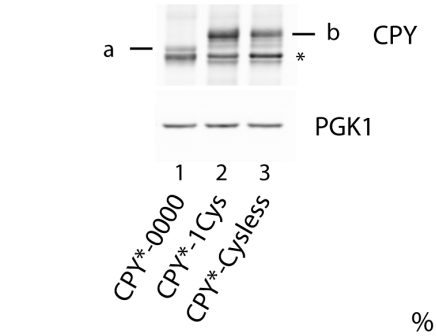

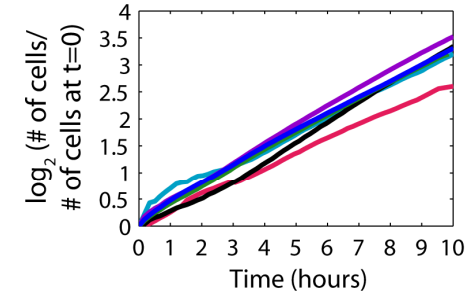

G

Construct	Strain	[$CuSO_4$]	% cells with eroGFP ratio>1 Median	Mean
Empty	WT	200	0.078	0.082
CPY			0.39	0.33
CPY*			5.9	5.7
Empty	hrd1Δ		0.40	0.63
CPY			4.1	4.2
CPY*			11	10
Empty	WT	500	0.55	0.51
CPY			3.4	3.7
CPY*			11	12
CPY*0000			15	16
CPY*-1cys			10	11
CPY*-Cysless			4.6	4.3

Figure S9. Characterization of copper-inducible CPY and CPY* variants

(A) Time courses of the eroGFP ratio and UPR-RFP histograms for wild-type and *hrd1*Δ cells expressing the composite reporter and empty vector treated with 200μM or 500μM copper sulfate. Color represents percentage of cells at a given metric value and time point. The dashed gray line signifies time of copper addition. (B) Immunoblot against HA and PGK1 of protein extracts from cells harboring empty vector, P_{CUP1}-CPY-HA, or P_{CUP1}-CPY*-HA in the presence and absence of 200μM copper sulfate. (C) Immunoblot against HA and PGK1 of protein extracts from cells treated with 200μM or 500μM copper sulfate. (D) Cells expressing P_{CUP1}-CPY*-HA were treated with 200μM copper sulfate at time, t=0 and samples were taken for immunoblot every 2 hours for 8 hours. (E) Immunoblot against CPY from cells expressing P_{CUP1}-CPY*0000, P_{CUP1}-CPY*-1cys, or P_{CUP1}-CPY*Cys-less treated with 200μM copper sulfate. The band marked "a" denotes unglycosylated CPY*, while "b" denotes glycoyslated CPY*. An * signifies a non-specific band. (F) Growth curves from experiments described in Figure 5 for wild-type cells treated with 500μM copper sulfate expressing the indicated CPY construct or empty vector. The color of the line denotes which construct was expressed (see G). (G) Summary of the percentage of cells in the deflected population from Figure 5 defined as cells with an eroGFP ratio greater than 1.

Supplementary Figure S10

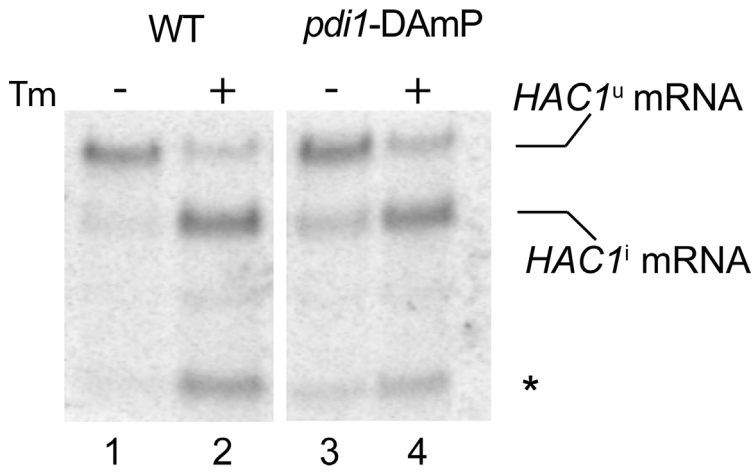

Figure S10. Increased UPR activity in a protein oxidation mutant in the absence of ER stress

Northern blot for *HAC1* mRNA for wild-type or *pdi1*-DAmP cells treated with or without tunicamycin (1μg/ml) for 1 hour. $HAC1^{u}$ denotes unspliced and $HAC1^{i}$ spliced mRNA respectively. An asterisk signifies the *HAC1* 5' exon. Percent spliced *HAC1* mRNA was calculated as $HAC1^{i}$ mRNA over $HAC1^{i} + HAC1^{u}$ mRNA. 28% greater splicing was evident in lane 3 vs. 1 (unstressed).

Supplementary Figure S11

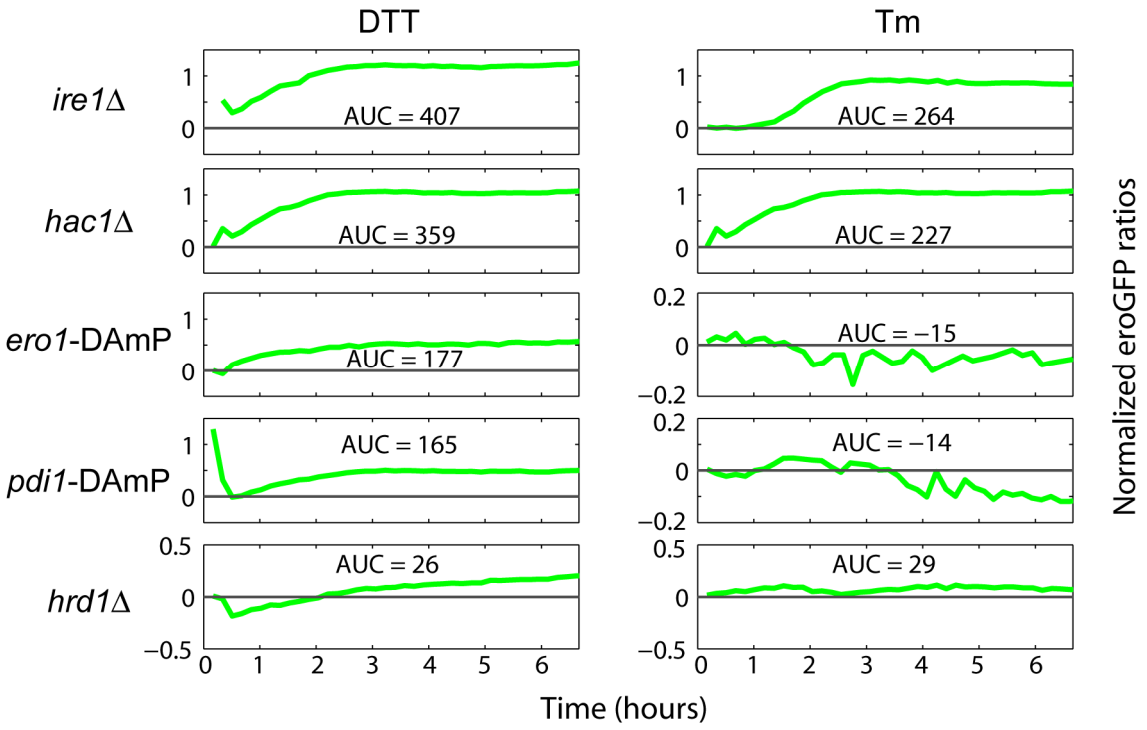

Figure S11. Normalized eroGFP ratios for ER oxidative folding, quality control, and UPR signaling mutants during pharmacologically-induced ER stress

Median values of the eroGFP ratio time courses for each mutant were normalized to wild-type. These normalized curves were then integrated over the time course with time, t= 0 denoting time of stressor addition, and reported as areas under the curves (AUC)

Supplementary Figure S12

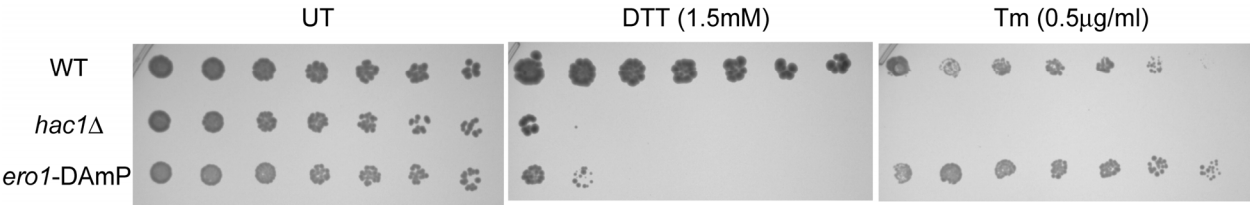

Figure S12. Differential growth for *ero1*-DAmP during protein oxidation and protein glycosylation stresses

Serial dilutions for wild-type, *hac1*Δ, and *ero1*-DAmP cells "frogged" onto synthetic-media plates without drug (UT), or with DTT (1.5mM) or Tm (0.5µg/ml). Image was taken 3 days after plating.

Supplementary Table S1

Strain	**Genotype**
YPM46	MAT**a**, *his3*Δ*1*, *leu2*Δ*0*, *met15*Δ*0*, *ura3*Δ*0*, eroGFP::NAT
YPM51	MAT**a**, *his3*Δ*1*, *leu2*Δ*0*, *met15*Δ*0*, *ura3*Δ*0*, eroGFP-UPR-RFP::NAT
YPM59	MAT**a**, *his3*Δ*1*, *leu2*Δ*0*, *met15*Δ*0*, *ura3*Δ*0*, *hrd1*Δ::KAN, eroGFP-UPR-RFP::NAT
YPM66	MAT**a**, *his3*Δ*1*, *leu2*Δ*0*, *met15*Δ*0*, *ura3*Δ*0*, *ire1*Δ::KAN, eroGFP-UPR-RFP::NAT
YPM67	MAT**a**, *his3*Δ*1*, *leu2*Δ*0*, *met15*Δ*0*, *ura3*Δ*0*, *hac1*Δ::KAN, eroGFP-UPR-RFP::NAT
YPM68	MAT**a**, *his3*Δ*1*, *leu2*Δ*0*, *met15*Δ*0*, *ura3*Δ*0*, *pdi1*-DAmP::NAT, eroGFP-UPR-RFP::KAN
YPM69	MAT**a**, *his3*Δ*1*, *leu2*Δ*0*, *met15*Δ*0*, *ura3*Δ*0*, *ero1*-DAmP::NAT, eroGFP-UPR-RFP::KAN
YPM70	MAT**a**, *his3*Δ*1*, *leu2*Δ*0*, *met15*Δ*0*, *ura3*Δ*0*, eroGFP(C147S)::NAT
YPM72	MAT**a**, *his3*Δ*1*, *leu2*Δ*0*, *met15*Δ*0*, *ura3*Δ*0*, GAL1-eroGFP::NAT